Modeling Hyperalgesia Treatment through Transcutaneous Electrical Nerve Stimulation

Andrew Pla
Department of Bioengineering
University of California, San Diego
La Jolla, CA 92093
apla@eng.ucsd.edu

Anthony Han
Department of Bioengineering
University of California, San Diego
La Jolla, CA 92093
abh014@eng.ucsd.edu

Abstract

Transcutaneous electrical nerve stimulation (TENS) has been commonly used for non-invasive pain relief in patients. Two potential mechanisms by which TENS induces analgesia are investigated: (1) opioid receptor activation (2) interruption of action potential propagation. Results indicate that opioid receptor activation significantly reduces pain signal activity through several biochemical pathways and mechanisms of action, while an applied electrical current with medium frequency (~20 Hz), high amplitude (≥ 30 $\mu A/cm^2$), and low duty cycles (≤ 10%) provided the most amount of impediment to pain signal propagation for the modeled neuron.

1 Introduction

Transcutaneous electrical nerve stimulation (TENS) is a non-invasive therapeutic application of electrical currents across a patient's skin using a portable pulse generator for analgesic purposes. TENS has been used for alleviating many different kinds of pain, including musculoskeletal, nociceptive, and neuropathic. TENS therapies are variable and can be adjusted in terms of the pulse width, frequency, and amplitude of the applied electrical currents [1]. Many of the postulated mechanisms of TENS are currently being investigated and parameters for TENS treatment still need to be optimized. This paper attempts to characterize and model the application of TENS for hyperalgesia treatment by studying two postulated mechanisms through which TENS is capable of inducing analgesia in patients. TENS is believed to produce analgesic effects through both opioid receptor activation and direct interference and interruption of action potential propagation of pain signals [2, 3].

The activation of opioid receptors triggers and influences several biochemical pathways in modalities akin to those arising from the administration of pain relieving drugs such as morphine. There are three types of opioid receptors: kappa, mu, and delta [4]. Pain relieving drugs such as morphine typically activate the mu receptors [5]. The downstream effects of opioid receptor activation are outlined in Figure 1. As can be seen, opioid receptor activation leads to increased efflux of potassium ions, decreased influx of calcium ions, and inhibition of adenylate cyclase (AC) [4]. Increased potassium efflux is expected to both shorten the action potential duration, due to increased repolarization and restoration rate of the membrane resting potential, as well as hyperpolarize the membrane potential due to positive ions leaving the cell interior, making the cell interior even more negatively charged relative to the cell exterior. On the other hand, decreased calcium influx and inhibition of AC activity are both expected to effectively inhibit excitatory neurotransmitter release from the synapse, thus preventing the pain signal from being able to propagate and be carried on over to the postsynaptic neuron [5].

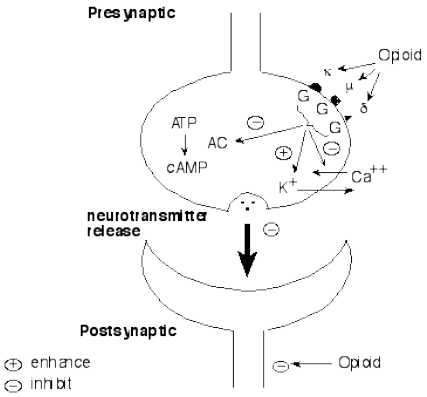

Figure 1: Overview of downstream effects of opioid receptor activation [5]

In order to investigate the direct interference and disruption of pain signal action potentials by TENS, the pulse width, frequency, and amplitude of the applied electrical currents are varied and evaluated in terms of how the propagation and reception of pain signals along an axon are affected. Furthermore, this potentially allows for the optimization of common parameters that often dictate TENS treatment efficacy, by identifying the most ideal combination of parameters that results in the greatest amount of pain signal disruption and attenuation.

1 Methods

Simulations were run in MATLAB using the full Hodgkin-Huxley (HH) model. A point neuron model was used to simulate the effects of opioid receptor activation since the primary focus was on changes in spiking dynamics and in the interactions between two point neurons in a simple excitatory neural junction. On the other hand, simulating the direct interference and disruption of action potentials required a modified version of the HH model that accounted for the propagation of action potentials in a neural axon model, which included additional considerations and variables such as the radius, length, and resistance of the axon.

1.1 Opioid Receptor Activation

As mentioned before, one of the effects of opioid receptor activation is that it increases potassium efflux out of the neuron. An HH point neuron model was used in order to focus on changes in the spiking dynamics and overall activity of action potentials in response to this increase. Looking at a typical action potential (Figure 2), it is expected that the increase in potassium efflux will increase the rate of repolarization of the membrane potential, thus resulting in a faster and steeper slope during the repolarization phase and a shorter action potential duration. In order to simulate the increased potassium efflux, the effective conductance of the neuron to potassium ions, $E_{K,}$ was increased from 36 → 100 mS/cm^2. This would in theory allow for more potassium ions to more easily cross the membrane and drive membrane repolarization even faster.

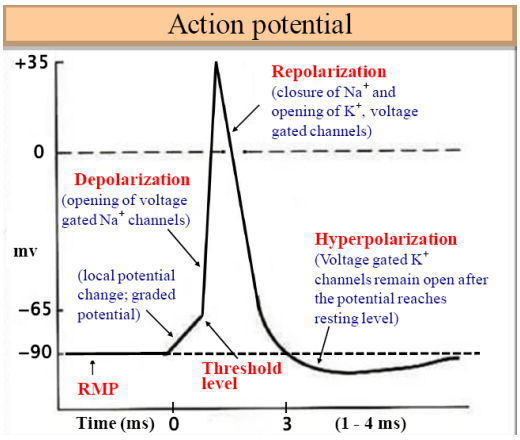

Figure 2: Phases in a typical action potential [6]

Opioid receptor activation also leads to decreased calcium ion influx and inhibition of AC activity, which ultimately hinders release of excitatory neurotransmitters and prevents the action potentials from propagating across multiple neurons. In order to model this phenomenon, a simple excitatory synapse was used to observe changes in the spiking relationship between the presynaptic and postsynaptic neurons. Calcium ions are essential for ensuring proper fusion of the neurotransmitter-filled vesicles with the synapse membrane and subsequent release of their cargo into the synaptic cleft. Thus blockage of N-type voltage-dependent calcium channels by opioids can hinder the influx of calcium ions into the neuron and the downstream processes that depend on it. Likewise, AC is responsible for converting adenosine triphosphate (ATP) into cyclic adenosine monophosphate (cAMP), which regulates many downstream pathways and molecules, such as cAMP-dependent protein kinase A (PKA), which also play crucial roles in ensuring the release of neurotransmitters from the synapse. Opioid-induced AC inhibition thus further works to prevent excitatory neurotransmitters from being released. In order to simulate these effects, the effective synaptic conductance to excitatory neurotransmitters, g_{GLU}, was decreased from 0.3 → 0.1 mS/cm^2. This would simulate the increased difficulty and lower levels of excitatory neurotransmitter release [4].

1.2 Interruption of Action Potential Propagation

An expanded version of the HH equation was used to model action potential movement down an unmyelinated axon. This equation adds a spatial component, turning the HH equation into a partial differential equation and allowing the propagation of the action potential to be modeled. The equation is as follows,

$$\frac{a}{2R}\frac{\partial^2 V}{\partial x^2} = C_m\frac{\partial V}{\partial t} + I_K + I_{Na} + I_L - I_{ext}$$

Where a is the radius of the axon (0.002cm), R is the axoplasmic resistance (90Ω*cm), C_m is the membrane capacitance (1μF/cm^2), and the other parameters are the standard HH equations [7]. In cases of high pain, sensory neurons are firing very frequently. This was translated into the model through a sinusoidal value boundary condition at x=0, which induces a regular action potential that propagates down the axon.

The goal of this simulation was to investigate how external current, applied by a TENS device, affects the regular action potentials of this nerve model. Specifically, the effects that varying frequency, amplitude, and duty cycle (percent of time that the current is 'on') have on action potential propagation. To this end, I_{ext} was modeled as a square wave with these three variable parameters. Each parameter was altered, one at a time, in order to see its individual effect. Key representative values for frequency were 10, 20, and 100 Hz; representative points for amplitude were 10, 30, and 50 μA/cm^2; and for duty cycle were 10%, 50%, and 100%.

2 Results

2.1 Opioid Receptor Activation

Simulating the increased potassium efflux, it could be observed that upon analysis of a single action potential (Figure 3), there was indeed an increase in the membrane repolarization rate in the opioid activated neuron (red) compared to that in the normal neuron (blue) as evident from the steeper repolarization slope. There was also a decrease in the action potential duration that could be observed from the shorter pulse width of the opioid activated action potential. Despite the normal action potential peaking at an earlier time point and hence beginning repolarization earlier, the opioid activated action potential still completes repolarization and reaches the resting membrane potential faster.

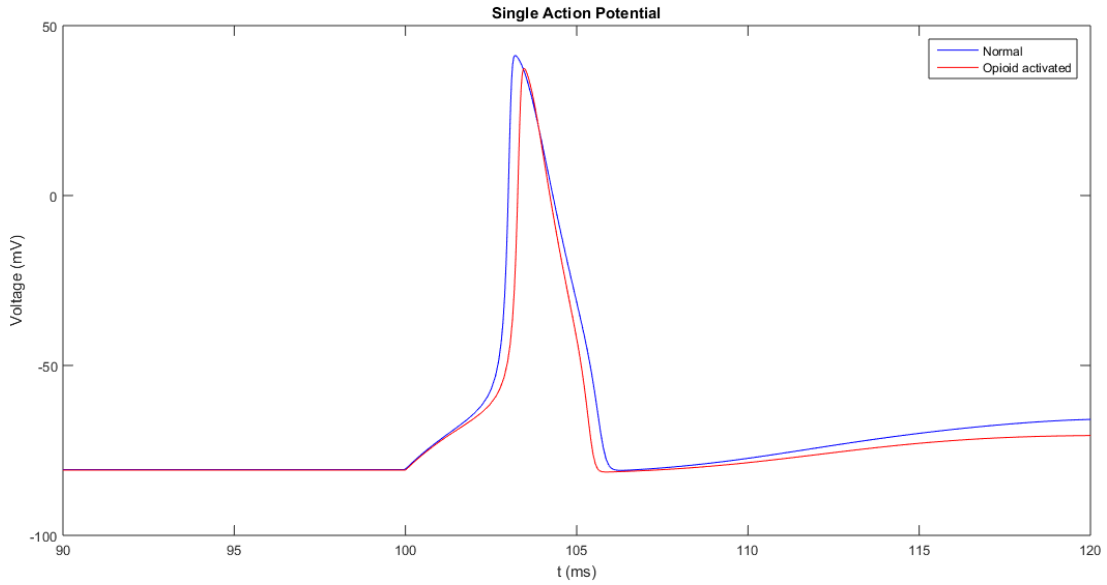

Figure 3: Comparison of a single action potential in an opioid activated and a normal neuron

Looking at the overall pain signal activity (Figure 4), results indicate that increased potassium efflux significantly reduces activity with a decrease in the spiking frequency. The combination of shorter action potential durations along with a general decrease in the number of action potentials that get initiated validate the analgesic effects produced from enhanced potassium efflux downstream of opioid receptor activation.

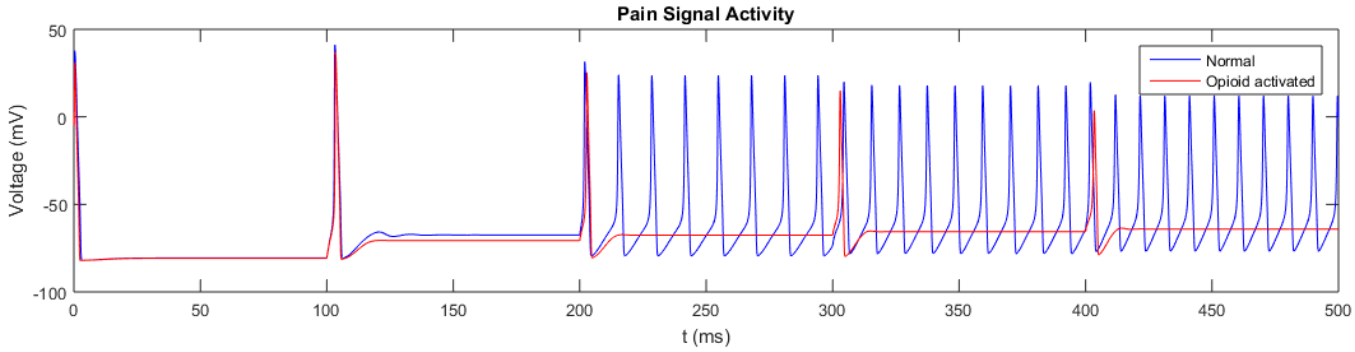

Figure 4: Comparison of a single action potential in an opioid activated and a normal neuron

Simulations ran for the inhibition of excitatory neurotransmitters due to decreased calcium influx and AC inhibition also show a different, robust analgesic effect of opioid receptor activation. Comparing a normal excitatory neural junction (Figure 5) to an opioid activated junction (Figure 6), there is clear inhibition of the pain action potential from propagating and getting transferred to the postsynaptic neuron in the case of the opioid activated junction. Even when the presynaptic neuron is assumed to have the same spiking dynamics, opioid activation leads to severe attenuation of the postsynaptic neuron's spiking capabilities due to the inability of the two neurons to communicate effectively.

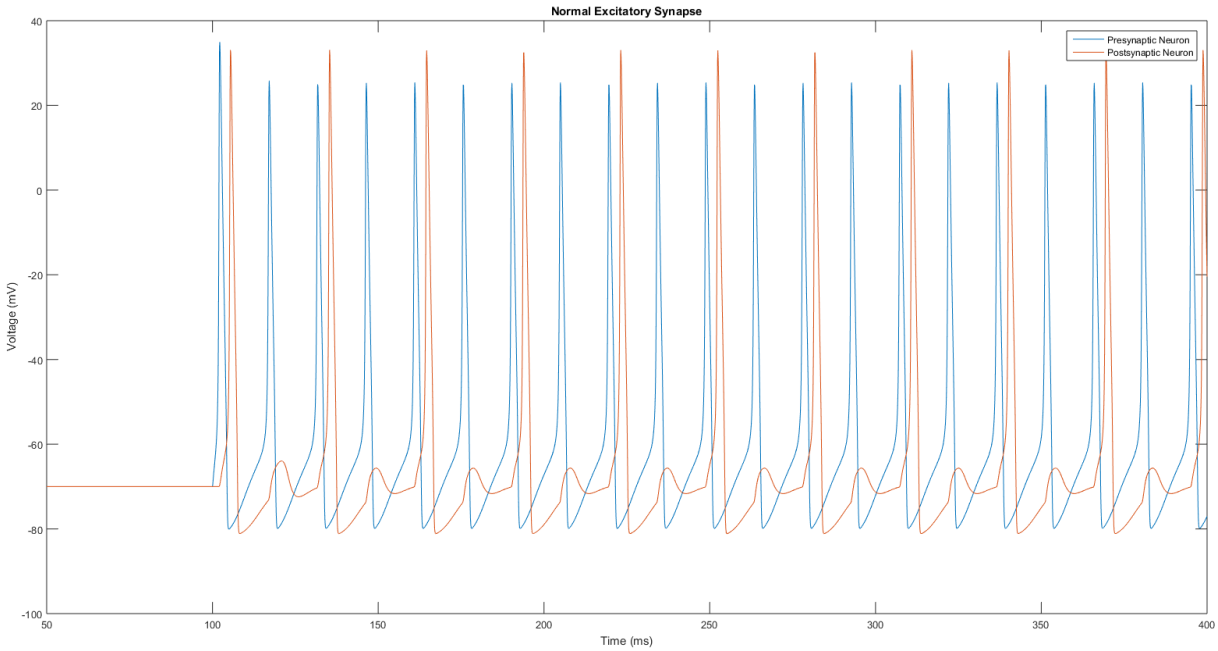

Figure 5: Spiking dynamics in a normal excitatory synapse
(presynaptic neuron-blue; postsynaptic neuron-red)

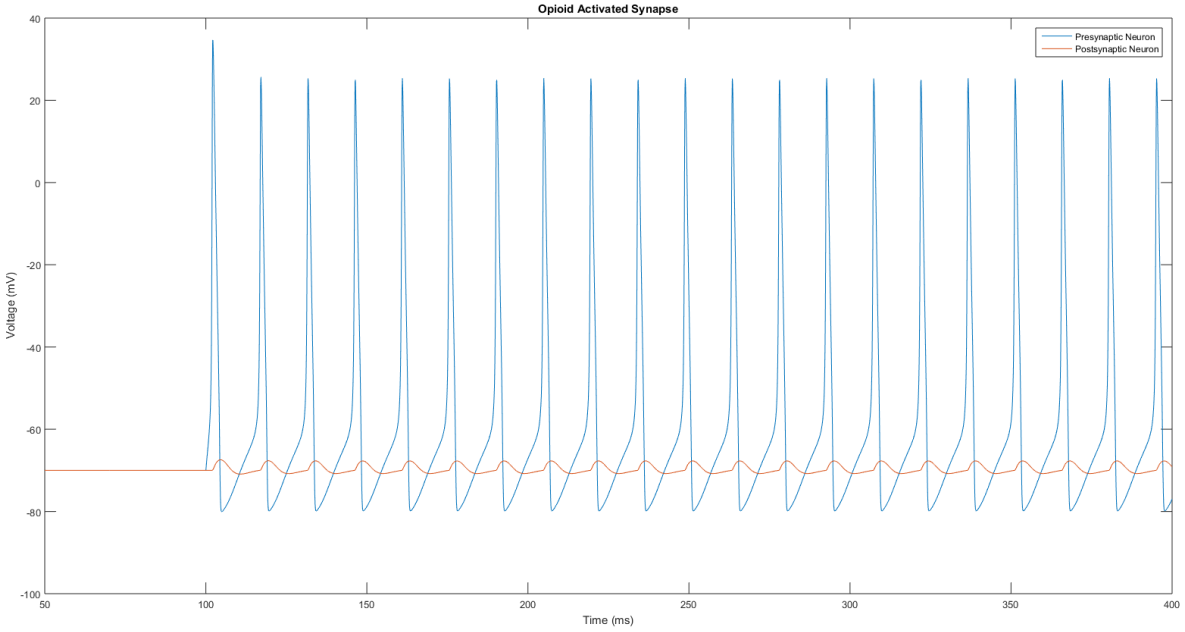

Figure 6: Spiking dynamics in an opioid activated excitatory synapse
(presynaptic neuron-blue; postsynaptic neuron-red)

2.2 Interruption of Action Potential Propagation

A firing neuron with no external current (Figure 7) was modeled first as a baseline comparison to neurons experiencing current from TENS. External current was then added to the model, and the first parameter examined was frequency (Figure 8). It can be seen that when the external current is affecting the axon, firing occurs along the entire length of the axon simultaneously, interrupting any potential that may have been travelling along the axon at the time. A low frequency (10 Hz, Figure 8a) results in interruptions infrequent enough to let many of the natural action potentials full propagate to the axon terminus. A higher frequency (20 Hz, Figure 8b) is sufficient to interrupt all of the natural action potentials and a very high frequency (100 Hz, Figure 8c) drowns out the natural signals, creating more potentials than it interrupts.

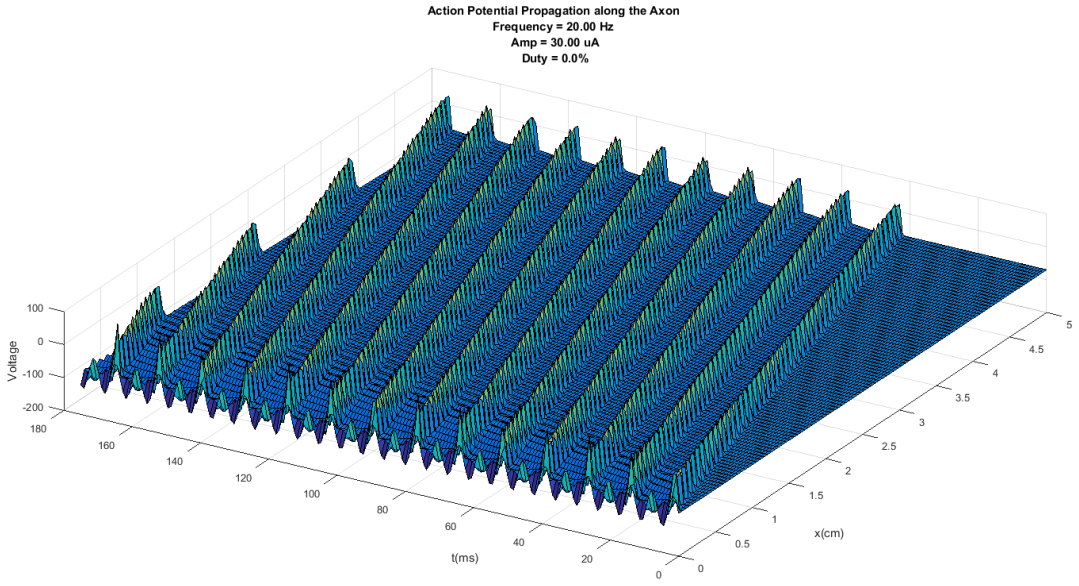

Figure 7: Natural action potential propagation down a rapidly firing neuron unaffected by TENS

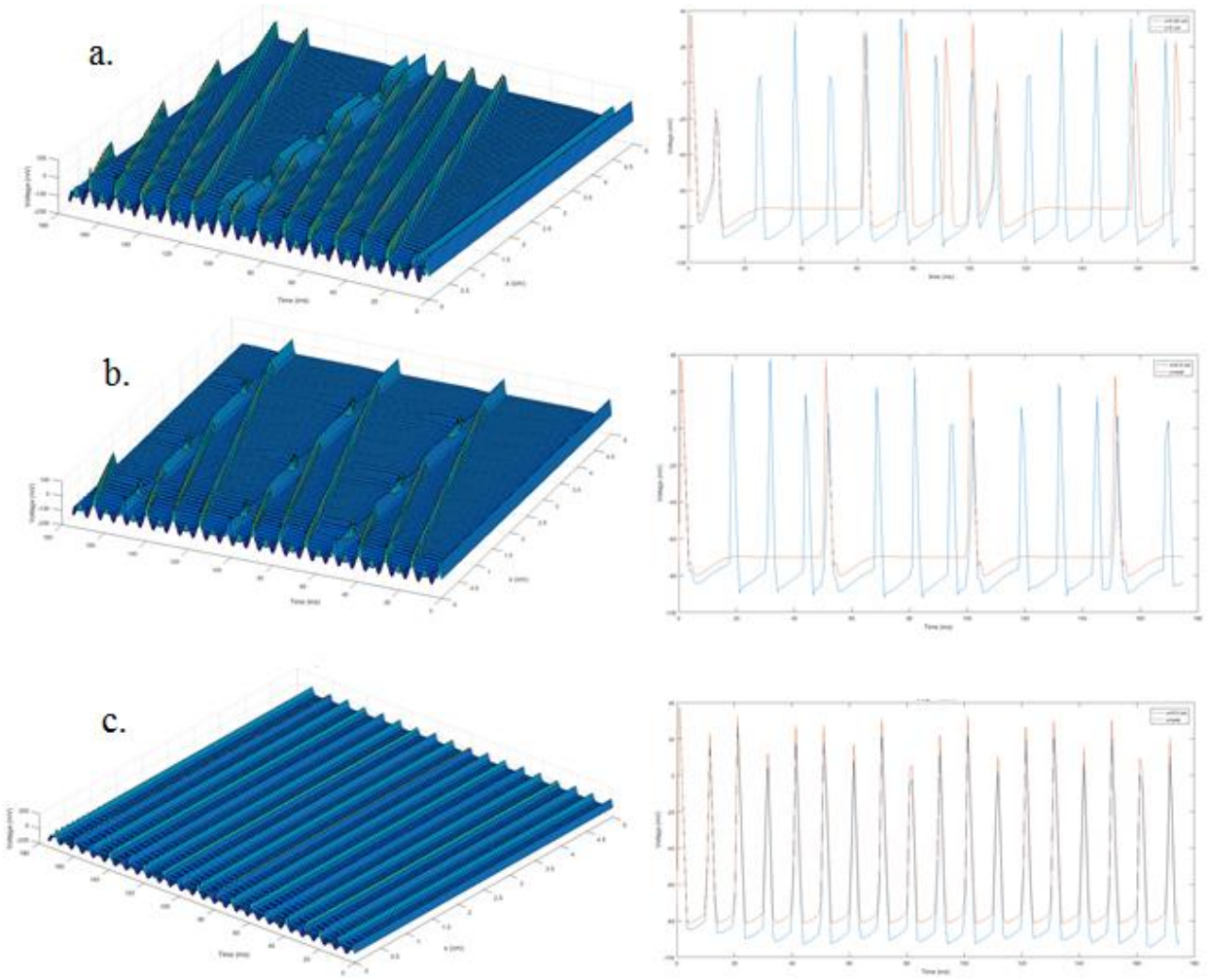

Figure 8: Neuron firing patterns for different frequencies. a) frequency = 10 Hz; b) frequency = 20 Hz; c) frequency = 100 Hz. Each neuron experiences an amplitude of 30 $\mu A/cm^2$ and duty cycle of 10%. On the left are the 3D plots of voltage against x (0 to 5 cm) and time (0 to 180 ms). On the right is shown the voltage just at the start of the axon (x=0.5 cm, blue) and at the axon terminal (x=5cm, red), in order to compare the action potential frequency at the beginning vs the action potential frequency reaching the axon terminal.

The next parameter of I_{ext} examined was amplitude (Figure 9). Here it can be seen that that a low amplitude (10 $\mu A/cm^2$, Figure 9a) is insufficient to trigger an action potential across the axon, and thus it is insufficient to interrupt any signals propagating down the axon; it delays the signals slightly, but nothing more. Increasing the amplitude (30 $\mu A/cm^2$, Figure 9b) sufficiently high results in proper interruption of signals and increasing the signal further still (50 $\mu A/cm^2$, Figure 9c) has no significant added effect. From this it can be surmised that a high amplitude or TENS intensity is desirable for maximum effectiveness.

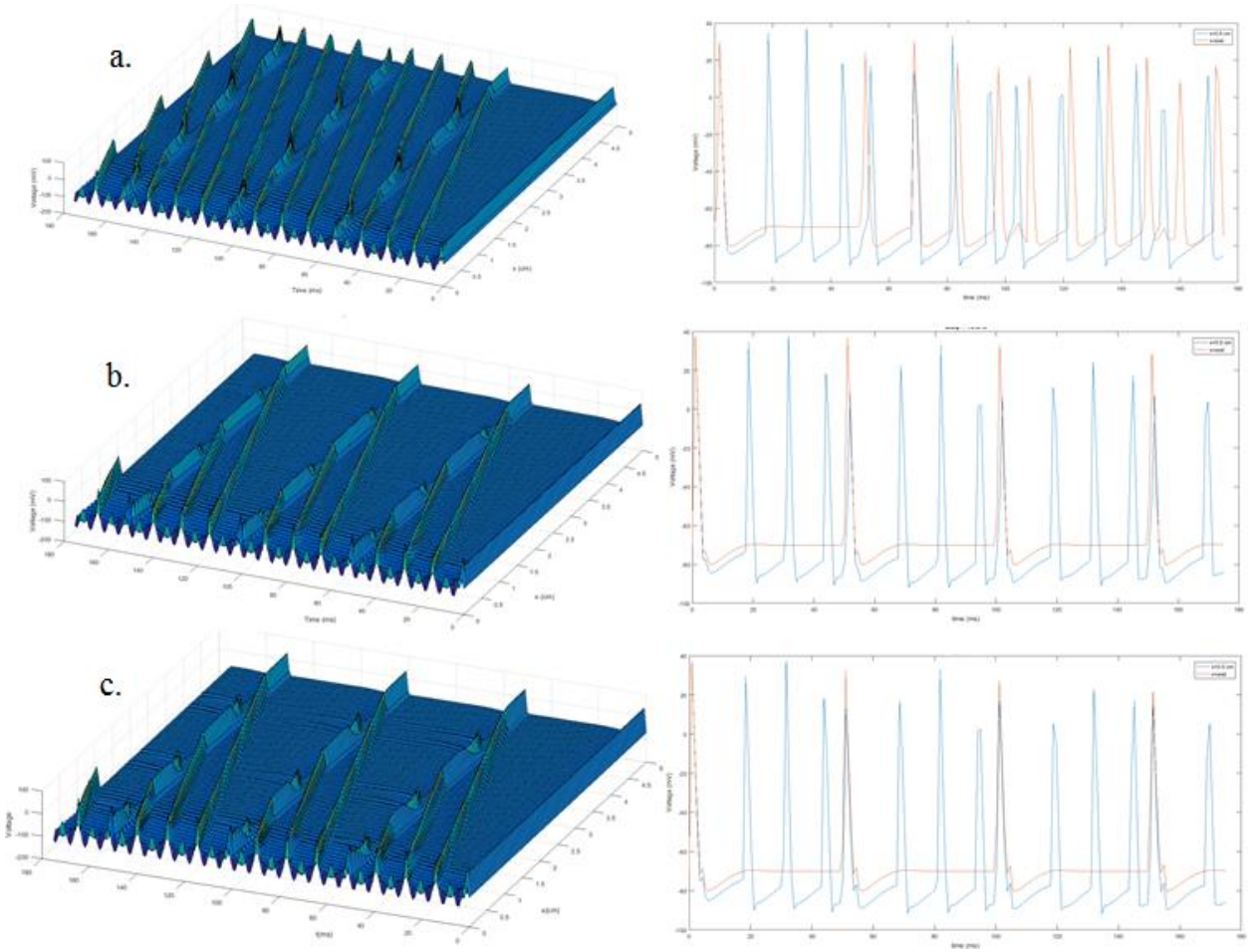

Figure 9: Neuron firing patterns for different amplitudes. a) amplitude = 10 μA/cm^2; b) amplitude = 30 μA/cm^2; c) amplitude = 50 μA/cm^2. Each neuron experiences a frequency of 20 Hz and duty cycle of 10%. On the left are the 3D plots of voltage against x (0 to 5 cm) and time (0 to 180 ms). On the right is shown the voltage just at the start of the axon (x=0.5 cm, blue) and at the axon terminal (x=5cm, red), in order to compare the action potential frequency at the beginning vs the action potential frequency reaching the axon terminal.

The final parameter examined was duty cycle, which is the percent of time that the external alternating current signal is on (Figure 10). At a low duty cycle (10%, Figure 10a) it was seen that the current was only on long enough to trigger one interrupting action potential in the axon. This produced maximum reduction in the frequency of action potentials reaching the axon terminal. As duty cycle increased (50%, Figure 10b; 100%, Figure 10c), repeated action potentials were triggered as long as the external current was on, resulting in a high frequency of action potentials at the axon terminal. This shows that a low duty cycle is ideal for minimizing the frequency of signals being transmitted by the neuron.

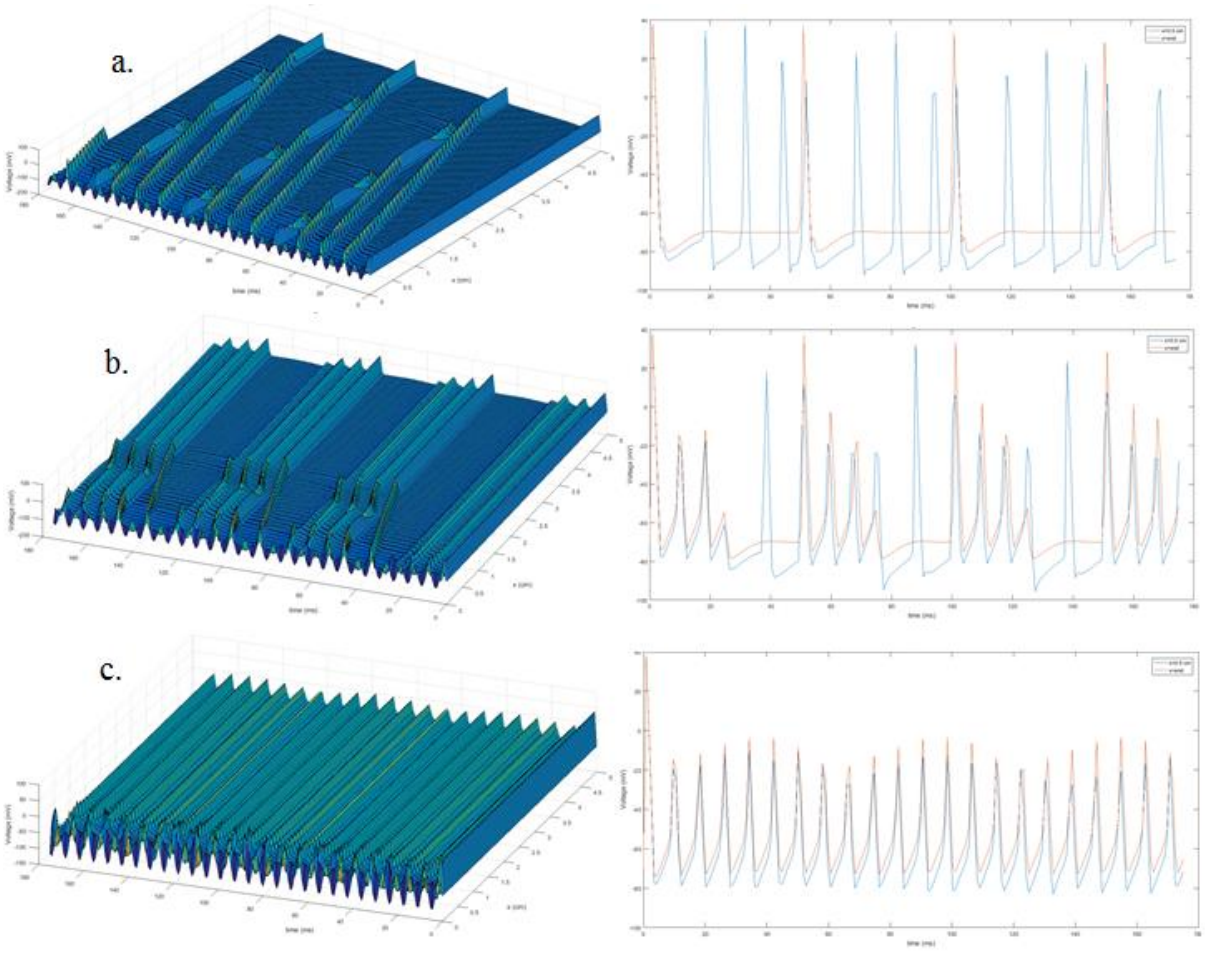

Figure 10: Neuron firing patterns for different duty cycles. a) duty cycle = 10%; b) duty cycle = 50%; c) duty cycle = 100%. Each neuron experiences a frequency of 20 Hz and amplitude of 30 μA/cm^2. On the left are the 3D plots of voltage against x (0 to 5 cm) and time (0 to 180 ms). On the right is shown the voltage just at the start of the axon (x=0.5 cm, blue) and at the axon terminal (x=5cm, red), in order to compare the action potential frequency at the beginning vs the action potential frequency reaching the axon terminal.

3 Conclusion

TENS has been shown to produce analgesia in patients in two distinct mechanisms of action. TENS stimulates opioid receptor activation, which leads to increased potassium efflux that drives faster repolarization and hyperpolarizes the membrane potential, decreasing the duration of individual pain signal action potentials and the overall pain signal activity and firing rate. Opioids also lead to decreased calcium influx and AC inhibition, which work to prevent excitatory neurotransmitter release, effectively hindering the propagation of pain signals across a neural network. On the other hand, TENS also directly interrupts pain action potential propagation down a neural axon. For the modeled neuron, the optimal parameters for maximal signal attenuation has been determined to be the administration of electrical currents with medium frequencies around 20 Hz, high amplitudes of $\geq$ 30 μA/cm^2, and low duty cycles of $\leq$ 10%. The range of parameters examined matched up with those seen in current TENS usage [1, 2]. It was also seen that the parameters could be altered to stimulate nerves instead of interrupting them, which could be useful for stimulating pain-relieving nerves. Future work, for example, may include further analysis of the variations in potency across the three different types of opioid receptors; action potential interruption in neurons of different radii, natural firing frequency, and/or conductivity; the efficacy of TENS in treating different types of pain; and the impact of neural plasticity on the analgesic effects of TENS in subsequent treatments.

References

[1] Enriched HealthCare, Physiotherapy & Exercise Physiology. “Use of TENS guidelines.” Accessed December 8, 2016. http://www.enrichedhealthcare.com.au/library/resources/tens

[2] Electrotherapy on the web. “Transcutaneous Electrical Nerve Stimulation.” Accessed December 5, 2016. http://www.electrotherapy.org/modality/transcutaneous-electrical-nerve-stimulation-tens

[3] DeSantana, J. Walsh, D., et al. “Effectiveness of Transcutaneous Electrical Nerve Stimulation for Treatment of Hyperalgesia and Pain.” Curr Rheumatol Rep. 2008 Dec; 10(6): 492–499

[4] Chahl, L. “Opioids – mechanisms of action.” Aust Prescr. 1996;19:63-5

[5] KA, S. MA, J. et al. “Low frequency TENS is less effective than high frequency TENS at reducing inflammation-induced hyperalgesia in morphine-tolerant rats.” Eur J Pain. 2000;4(2):185-93.

[6] howMed. “Action Potential.” Accessed December 2, 2016. http://howmed.net/physiology/action-potential/

[7] Hodgkin, A.L., Huxley, F. “A Quantitative Description of Membrane Current and its Application to Conduction and Excitation in Nerve.” J. Phisiol. 1952; 117:500-544.

Appendix A: Code for Mechanism 1

```
%% BENG 260 Neurodynamics Project: Transcutaneous Electrical Nerve Stimulation (TENS)

%% Mechanism 1: Opioid Activation
%Point Model (Full H-H model)

% Constants
C_m  =   1.0; % membrane capacitance, in uF/cm^2
g_Na = 120.0; % maximum conducances, in mS/cm^2
g_K  =  36.0;
g_L  =   0.3;
E_Na =  115.0; % Nernst reversal potentials, in mV
E_K  = -12.0;
E_L  = -10.613;
t=[0:500]; %ms

% Channel gating kinetics
% Rate Functions (Resting membrane potential = -70 mV)
alpha_m = @(V) 0.1.*(V+45.0)./(1.0 - exp(-(V+45.0) ./ 10.0));
beta_m  = @(V) 4.0.*exp(-(V+70.0) ./ 18.0);
alpha_h = @(V) 0.07.*exp(-(V+70.0) ./ 20.0);
beta_h  = @(V) 1.0./(1.0 + exp(-(V+40.0) ./ 10.0));
alpha_n = @(V) 0.01.*(V+60.0)./(1.0 - exp(-(V+60.0) ./ 10.0));
beta_n  = @(V) 0.125.*exp(-(V+70) ./ 80.0);

% Membrane currents (in uA/cm^2)
I_Na = @(V,m,h) g_Na .* m.^3 .* h .* (V+70 - E_Na);
I_K  = @(V, n)  g_K  .* n.^4      .* (V+70 - E_K);
I_L  = @(V)     g_L               .* (V+70 - E_L);

% step up 10 uA/cm^2 every 100ms
I_ext = @(t) 10 .* floor(t ./ 100);


% vector coding of state variables: X = [V, m, h, n]
dVmdt = @(t, X) [
    (I_ext(t) - I_Na(X(1), X(2), X(3)) - I_K(X(1), X(4)) - I_L(X(1))) / C_m;  % dV / dt
    alpha_m(X(1))*(1.0-X(2)) - beta_m(X(1))*X(2);  % dm / dt
    alpha_h(X(1))*(1.0-X(3)) - beta_h(X(1))*X(3);  % dh / dt
    alpha_n(X(1))*(1.0-X(4)) - beta_n(X(1))*X(4);  % dn / dt
    ];

[t, X] = ode23(dVmdt, [0 500], [0 0.05 0.6 0.32]);

V = X(:,1);
m = X(:,2);
h = X(:,3);
n = X(:,4);

%INCREASED K+ Efflux (36 --> 100 mS/cm^2)
C_m  =   1.0; % membrane capacitance, in uF/cm^2
g_Na = 120.0; % maximum conducances, in mS/cm^2
g_K  =  80.0;
g_L  =   0.3;
E_Na =  115.0; % Nernst reversal potentials, in mV
E_K  = -12.0;
E_L  = -10.613;
t1=[0:500]; %ms

% Channel gating kinetics
% Rate Functions (Resting membrane potential = -70 mV)
alpha_m = @(V) 0.1.*(V+45.0)./(1.0 - exp(-(V+45.0) ./ 10.0));
beta_m  = @(V) 4.0.*exp(-(V+70.0) ./ 18.0);
alpha_h = @(V) 0.07.*exp(-(V+70.0) ./ 20.0);
beta_h  = @(V) 1.0./(1.0 + exp(-(V+40.0) ./ 10.0));
alpha_n = @(V) 0.01.*(V+60.0)./(1.0 - exp(-(V+60.0) ./ 10.0));
beta_n  = @(V) 0.125.*exp(-(V+70) ./ 80.0);

% Membrane currents (in uA/cm^2)
I_Na = @(V,m,h) g_Na .* m.^3 .* h .* (V+70 - E_Na);
I_K  = @(V, n)  g_K  .* n.^4      .* (V+70 - E_K);
```

```
I_L  = @(V)     g_L               .* (V+70 - E_L);

% step up 10 uA/cm^2 every 100ms
I_ext = @(t) 10 .* floor(t ./ 100);


% vector coding of state variables: X = [V, m, h, n]
dVmdt = @(t1, X) [
    (I_ext(t1) - I_Na(X(1), X(2), X(3)) - I_K(X(1), X(4)) - I_L(X(1))) / C_m;  % dV / dt
    alpha_m(X(1))*(1.0-X(2)) - beta_m(X(1))*X(2);  % dm / dt
    alpha_h(X(1))*(1.0-X(3)) - beta_h(X(1))*X(3);  % dh / dt
    alpha_n(X(1))*(1.0-X(4)) - beta_n(X(1))*X(4);  % dn / dt
    ];

[t1, X] = ode23(dVmdt, [0 500], [0 0.05 0.6 0.32]);

V1 = X(:,1);
m = X(:,2);
h = X(:,3);
n = X(:,4);


figure();
plot(t,V,'b', t1, V1, 'r');
title('Single Action Potential')
xlim([90,120]);
xlabel('t (ms)');
ylabel('Voltage (mV)');
legend('Normal','Opioid activated');

figure();
subplot(2,1,1);
plot(t,V,'b', t1, V1, 'r');
title('Pain Signal Activity')
ylabel('Voltage (mV)');
xlabel('t (ms)');
legend('Normal','Opioid activated');

subplot(2,1,2);
plot(t, I_ext(t), 'k');
xlabel('t (ms)');
ylabel('I_{ext} (\mu{A}/cm^2)');

%% Neurotransmitter release inhibition

% Constants
C_m  =   1.0; % membrane capacitance, in uF/cm^2
g_Na = 120.0; % maximum conducances, in mS/cm^2
g_K  =  36.0;
g_L  =   0.3;
E_Na =  45.0; % Nernst reversal potentials, in mV
E_K  = -82.0;
E_L  = -59.387;
E_Cl = -80.0; % inhibitory synapse
E_ex = -38.0; % excitatory synapse

% Channel gating kinetics
% Functions of membrane voltage
alpha_m = @(V) 0.1.*(V+45.0)./(1.0 - exp(-(V+45.0) ./ 10.0));
beta_m  = @(V) 4.0.*exp(-(V+70.0) ./ 18.0);
alpha_h = @(V) 0.07.*exp(-(V+70.0) ./ 20.0);
beta_h  = @(V) 1.0./(1.0 + exp(-(V+40.0) ./ 10.0));
alpha_n = @(V) 0.01.*(V+60.0)./(1.0 - exp(-(V+60.0) ./ 10.0));
beta_n  = @(V) 0.125.*exp(-(V+70) ./ 80.0);

% Alpha / Beta constants for inhibitory / excitatory synapses
alpha_r_i = 5.0;  % 1/(mM*ms)
beta_r_i  = 0.18; % 1/ms
alpha_r_e = 2.4;  % 1/(mM*ms)
beta_r_e  = 0.56; % 1/ms
```

```
% [T] equation for synapses
T_max_i = 1.5; % mM (inhibitory)
T_max_e = 1.0; % mM (excitatory)
K_p = 5.0; % mV
V_p = 7.0; % mV
T_i = @(V_pre) T_max_i ./ (1.0 + exp(-(V_pre - V_p)./K_p));
T_e = @(V_pre) T_max_e ./ (1.0 + exp(-(V_pre - V_p)./K_p));

% Differential gating equations
dm = @(V,m) alpha_m(V).*(1.0-m)-beta_m(V).*m;
dh = @(V,h) alpha_h(V).*(1.0-h)-beta_h(V).*h;
dn = @(V,n) alpha_n(V).*(1.0-n)-beta_n(V).*n;
dr_i = @(V,r) alpha_r_i.*T_i(V).*(1.0-r)-beta_r_i.*r; % V=V_pre, r is for pre
dr_e = @(V,r) alpha_r_e.*T_e(V).*(1.0-r)-beta_r_e.*r; % V=V_pre, r is for pre

% Membrane currents (in uA/cm^2)
I_Na = @(V,m,h) g_Na .* m.^3 .* h .* (V - E_Na);
I_K  = @(V, n)  g_K  .* n.^4      .* (V - E_K);
I_L  = @(V)     g_L               .* (V - E_L);
I_syn_i = @(V,g_GABA,r) r*g_GABA.*(V-E_Cl); % V=V_post, r is for pre
I_syn_e = @(V,g_Glu,r)  r*g_Glu .*(V-E_ex); % V=V_post, r is for pre

% Membrane voltage differential
dV = @(V, m, h, n, r_i, r_e, I_ext, g_GABA, g_Glu) ...
    (-I_Na(V,m,h)-I_K(V,n)-I_L(V)-I_syn_i(V,g_GABA,r_i)-I_syn_e(V,g_Glu,r_e)+I_ext) ./ C_m;


% Setup ODE
d_single = @(t, x, I_ext, g_GABA, g_Glu) ...
    [ ...
    dV(x(1,:),x(2,:),x(3,:),x(4,:),x(5,:),x(6,:),I_ext(t),g_GABA,g_Glu); ...
    dm(x(1,:),x(2,:));   ...
    dh(x(1,:),x(3,:));   ...
    dn(x(1,:),x(4,:));   ...
    dr_i(x(1,:),x(5,:)); ...
    dr_e(x(1,:),x(6,:))];

% Run the differential equations for many neurons
d = @(t, x, I_exts, g_GABA, g_Glu) ...
    reshape(d_single(t, reshape(x, 6, length(x)/6), I_exts, g_GABA, g_Glu), length(x), 1);

% Shortcut for simulating a whole network
T = linspace(0, 500, 5000); % each division is 0.1 ms
network = @(I_exts, g_GABA, g_Glu) ...
    ode45(d, T, zeros(1, size(g_GABA, 1).*6), [], I_exts, g_GABA, g_Glu);



% Neuron A gets a 10 uA pulse from 100-400ms, the other neuron gets nothing
I_exts_ = [10 0]; % uA/cm^2
I_exts = @(t) I_exts_ .* (100<t&t<400);

% g_GABA is all zero, g_Glu is all A->B
g_Glu = [0 0.3; 0 0]; % mS/cm^2

% Normal Excitatory Synapse: g_Glu = 0.3 mS/cm^2
[t,v] = network(I_exts, [0 0; 0 0], g_Glu);
v = v';
V = v(1:6:end,:);
figure;
plot(t(501:4000), V(:,501:4000)); % from 50 to 450ms
title('Normal Excitatory Synapse');
xlabel('Time (ms)');
ylabel('Voltage (mV)');
legend('Presynaptic Neuron','Postsynaptic Neuron');

% g_GABA is all zero, g_Glu is all A->B
g_Glu = [0 0.1; 0 0]; % mS/cm^2 (g_Glu = 0.3 --> 0.1 mS/cm^2)

% Excitatory Neurotransmitter Release Inhibition: g_Glu = 0.1 mS/cm^2
[t,v] = network(I_exts, [0 0; 0 0], g_Glu);
```

```
v = v';
V = v(1:6:end,:);
figure;
plot(t(501:4000), V(:,501:4000)); % from 50 to 450ms
title('Opioid Activated Synapse');
xlabel('Time (ms)');
ylabel('Voltage (mV)');
legend('Presynaptic Neuron','Postsynaptic Neuron');
```

Appendix B: Code for Mechanism 2

```
%% BENG 260 Neurodynamics Project: Transcutaneous Electrical Nerve Stimulation (TENS)

%% Mechanism 2: Action Potential Propagation Interruption
% Note: Code takes some time to run but it is working

clear all
close all
clc

% Iext parameters: modify these
global freq amp duty
freq = 10; % Hz
amp = 30;
duty = 10; % Percent of time the wave is 'on'

xmesh = linspace(0,5,101);
tmesh = linspace(0,175,200);
%% Solve the system of 4 HH PDE/ODE
sol = pdepe(0,@pdefun,@ic,@bc,xmesh,tmesh);

V = sol(:,:,1)-70;

% 3D Plot of result
figure
surf(xmesh,tmesh,V)%,'EdgeColor','none');
xlabel('x(cm)')
ylabel('t(ms)')
zlabel('Voltage')
titstring = sprintf('Action Potential Propagation along the Axon \nFrequency = %.2f Hz \n Amp =
%.2f uA \nDuty = %.1f%%',freq,amp,duty);
title(titstring)

% 2D Plot at start of axon and end
figure
plot(tmesh,V(:,11),tmesh,V(:,end))
xlabel('time (ms)')
ylabel('Voltage (mV)')
titstr = sprintf('Voltage at beginning end of axon \nFrequency = %.2f Hz \n Amp = %.2f uA \nDuty
= %.1f%%',freq,amp,duty);
title(titstr)
legstr = sprintf('x=%.2f cm',0.5);
legend(legstr,'x=5 cm')

%% Run the simulation multiple times at different frequencies

% for freq = [10 20 100]
% sol = pdepe(0,@pdefun,@ic,@bc,xmesh,tmesh);
%
% V = sol(:,:,1)-70;
% % Plotting Data
%
% figure
% surf(xmesh,tmesh,V)%,'EdgeColor','none');
% xlabel('x (cm)')
% ylabel('Time (ms)')
% zlabel('Voltage (mV)')
% titstring = sprintf('Frequency = %.2f Hz\n Amp = %.2f uA \nDuty = %.1f%%',freq,amp,duty);
% title(titstring)
%
% figure
% plot(tmesh,V(:,11),tmesh,V(:,end))
% xlabel('Time (ms)')
% ylabel('Voltage (mV)')
% titstring = sprintf('Voltage at Beginning and End of Axon \nFrequency = %.2f Hz \n Amp = %.2f
uA \nDuty = %.1f%%',freq,amp,duty);
% title(titstring)
% legend('x=0.5 cm','x=end')
% end
%
%% Run the simulation multiple times at different amplitudes
```

```
% freq = 20; % Hz
% duty = 10; % Percent of time the wave is 'on'
%
% for amp = [10 30 50]
% sol = pdepe(0,@pdefun,@ic,@bc,xmesh,tmesh);
%
% V = sol(:,:,1)-70;
% % Plotting Data
%
% figure
% surf(xmesh,tmesh,V)%,'EdgeColor','none');
% xlabel('x (cm)')
% ylabel('Time (ms)')
% zlabel('Voltage (mV)')
% titstring = sprintf('Frequency = %.2f Hz\n Amp = %.2f uA\nDuty = %.1f%%',freq,amp,duty);
% title(titstring)
%
% figure
% plot(tmesh,V(:,11),tmesh,V(:,end))
% xlabel('time (ms)')
% ylabel('Voltage (mV)')
% titstring = sprintf('Voltage at Beginning and End of Axon \nFrequency = %.2f Hz \n Amp = %.2f
uA \nDuty = %.1f%%',freq,amp,duty);
% title(titstring)
% legend('x=0.5 cm','x=end')
% end

%% Run the simulation multiple times at different frequencies
% freq = 20; % Hz
% amp = 30;
%
% for duty = [10 50 100]
% sol = pdepe(0,@pdefun,@ic,@bc,xmesh,tmesh);
%
% V = sol(:,:,1)-70;
%
% % Plotting Data
%
% figure
% surf(xmesh,tmesh,V)%,'EdgeColor','none');
% xlabel('x (cm)')
% ylabel('time (ms)')
% zlabel('Voltage (mV)')
% titstring = sprintf('Frequency = %.2f Hz\n Amp = %.2f uA \nDuty = %.1f%%',freq,amp,duty);
% title(titstring)
%
% figure
% plot(tmesh,V(:,11),tmesh,V(:,end))
% xlabel('time (ms)')
% ylabel('Voltage (mV)')
% titstring = sprintf('Voltage at Beginning and End of Axon \nFrequency = %.2f Hz \n Amp = %.2f
uA \nDuty = %.1f%%',freq,amp,duty);
% title(titstring)
% legend('x=0.5 cm','x=end')
% end
%% PDEPE FUNCTIONS
function [c, f, s] = pdefun(x,t,u,DuDx)
% Constants
C = 1; % membrance capacitance (uF/cm^2)
R = 90; % axoplasmic resistance (ohm*cm)
a = .002; % radius of nerve (cm)
ENa = 115; % mV
EK = -12; % mV
EL = 10.613; % mV
gNa = 120; % mS/cm^2
gK = 36; % mS/cm^2
gL = 0.3; % mS/cm^2

% Define Iext as a square wave. Function of its parameters and time.
global freq amp duty
% Convert frequency from cycles/sec to cycles/ms
```

```
freq_ms = freq/1000;
Iext = @(t,freq_ms,amp,duty) amp + amp*square(2*pi*freq_ms*t,duty); % uA/cm^2
Iext1 = Iext(t,freq_ms,amp,duty);

% Defining the source terms for V, m, h, and n
% [u(1)=V   u(2)=m   u(3)=h   u(4)=n]
dvdts = (Iext1 - gNa.*u(2)^3.*u(3).*(u(1)-ENa) - gK.*u(4)^4.*(u(1)-EK) - gL.*(u(1)-EL));
dmdts = ((25-u(1))./(10*(exp((25-u(1))./10)-1)))  .*(1-u(2))  - 4*exp(-u(1)./18)
.*u(2);
dhdts = (0.07*exp(-u(1)./20))                     .*(1-u(3))  - (1./(exp((30-u(1))./10)+1))
.*u(3);
dndts = (10-u(1))./(100*(exp((10-u(1))./10)-1))   .*(1-u(4))  - 0.125*exp(-u(1)./80)
.*u(4);

c = [C;1;1;1];
f = [a/(2*R)*DuDx(1);0;0;0];
s = [dvdts;dmdts;dhdts;dndts];
end

function u0 = ic(x)
    u0 = [0;.05;.6;.32];
end

function [pl,ql,pr,qr] = bc(xl,ul,xr,ur,t)
    pl = [ul(1)-(sin(t)*50);0;0;0]; % Left boundary condition for voltage is a sin wave,
resulting in constant repeated firing of the neuron
    ql = [0;1;1;1];
    pr = [0;0;0;0];
    qr = [1;1;1;1];
end
```